Testing Time-Reversal Symmetry Using ^{199}Hg

J. P. Jacobs,* W. M. Klipstein, S. K. Lamoreaux, B. R. Heckel, and E. N. Fortson
Department of Physics, FM-15, University of Washington, Seattle, Washington 98195
(Received 25 May 1993)

A new search for a permanent electric dipole moment of ^{199}Hg has yielded the null result $d(^{199}\mathrm{Hg}) = -(2.7 \pm 5.8) \times 10^{-28} e\,\mathrm{cm}$ where the statistical and systematic uncertainty have been combined. This gives an upper limit of $d(^{199}\mathrm{Hg}) < 1.3 \times 10^{-27} e\,\mathrm{cm}$ (95% confidence). The measurement sets the most stringent limits to date on several possible sources of time-reversal symmetry violation. We look for a relative shift in Larmor-precession frequency between two optically pumped ^{199}Hg atomic oscillators in the presence of applied electric fields. We have attained a statistical uncertainty on the relative shift in frequency between the oscillators of 2×10^{-9} Hz.

PACS numbers: 35.10.Di, 11.30.Er, 32.80.Bx, 35.10.Wb

An isolated elementary particle or atomic system can possess a permanent electric dipole moment (EDM) only through some interaction which violates both parity conservation (P) and time-reversal symmetry (T). The existence of such an interaction is implied by the long-standing observation of CP violation in K_0 decay [1]. Recent EDM experiments have yielded null results for the neutron [2,3], for mercury, thallium, and cesium atoms [4–6], and for the thallium-fluoride molecule [7]. Each of these experiments is sensitive to certain sources of T violation, and taken together test T symmetry on a broad front [8,9]. We report here the results of a new experiment on the ^{199}Hg atom, which improves by over a factor of 25 the EDM limit set by our earlier mercury measurement [4], and sets new bounds on T-violating quark-quark and electron-quark interactions and on T violation in supersymmetric models [9].

The new version of our experiment has four major improvements: incorporation of a transverse pumping scheme which eliminates frequency shifts due to the pump light, stabilization of the Hg density and the spin relaxation time of the optical pumping cells, elimination of the most serious magnetic perturbation by reducing the leakage currents across the cells to the pA level, and an increase in signal by using enriched ^{199}Hg rather than natural Hg in the cells. The measurement is now sensitive to nHz frequency shifts, the smallest energy shift that has ever been detected in any experiment. Likewise, the limit on the ^{199}Hg EDM reported here is the smallest that has been set thus far on any system.

In the ground state of ^{199}Hg (6^1S_0) only the nuclear spin ($I = 1/2$) contributes to the total angular momentum. In external electric and magnetic fields $\mathbf{E}$ and $\mathbf{B}$ the Hamiltonian is

$$H = -(d\mathbf{E} + \mu\mathbf{B}) \cdot \mathbf{I}/I\,, \tag{1}$$

where d and μ are the electric and magnetic dipole moments. The violation of T in Eq. (1) is evident, since $\mathbf{E}$ does not change sign under $t \to -t$ whereas $\mathbf{B}$ and $\mathbf{I}$ both do.

We compare the ^{199}Hg Larmor-precession frequencies in two adjacent cells having equal but oppositely directed applied electric fields and the same magnetic field. From Eq. (1), an EDM would cause a frequency shift of $2Ed/h$ in each cell. The magnitude of the EDM is given by

$$d = \frac{h\delta\nu}{4E}, \tag{2}$$

where $\delta\nu$ is the difference in precession frequency between the two cells and h is Planck's constant. To extract d, we measure the change in $\delta\nu$ as $\mathbf{E}$ in each cell is reversed. Magnetic field shifts common to the two cells cancel, leaving the system magnetically sensitive only to changes in the magnetic field *gradient*.

The overall geometry of the apparatus is shown in Fig. 1. The EDM cells are positioned within three layers of magnetic shielding with a total shielding factor of about 70 000. Each cell functions as an optically pumped oscillator based on the Larmor-precession frequency of the nuclear spins about $B\hat{\mathbf{z}}$ (with $B \approx 10$ mG). The 253.7 nm line from a ^{204}Hg electrodeless-microwave-discharge lamp supplies the pumping radiation to polarize the nuclear

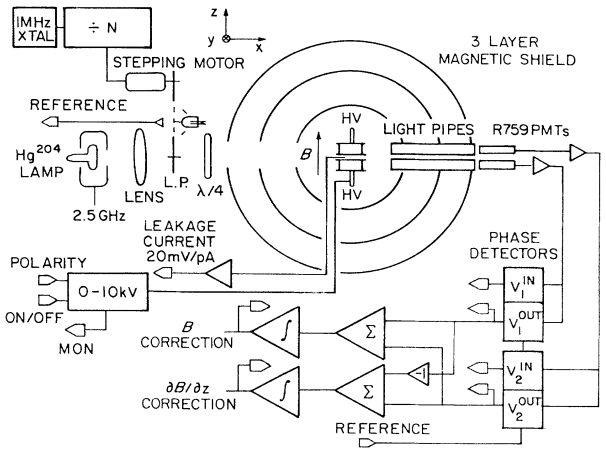

FIG. 1. ^{199}Hg EDM experiment block diagram.

0031-9007/93/71(23)/3782(4)$06.00

spins and monitor their precession. The pumping light is directed along $\hat{\mathbf{x}}$ and acquires a modulated circular polarization of form $P_x = P\cos\omega t$ by passage through a rotating linear polarizer (LP) followed by a fixed quarter-wave retardation plate ($\lambda/4$) (in some data the LP was fixed and the $\lambda/4$ plate rotated).

When ω is set close to the Larmor spin precession frequency ω_L, the optical pumping due to P_x causes a synchronized nuclear spin polarization, $\langle\mathbf{I}\rangle/I$, to build up to a steady state magnitude. $\langle\mathbf{I}\rangle$ rotates in the x-y plane with an x component given by $\langle I_x\rangle = |\langle\mathbf{I}\rangle|\cos(\omega t + \phi)$ [10–12]. A shift in the phase difference ϕ is a sensitive measure of any shift in ω_L, the Larmor spin precession frequency. The absorption of the polarized light depends upon $\langle I_x\rangle P_x$, producing a modulation in the transmitted light intensity at 2ω. The phase shift in this signal is used to measure the shift in precession frequency that would be caused by the coupling of an EDM to the electric field. Typically the 2ω modulation depth is approximately 15% of the total transmitted light intensity (with about 20% of the total light being nonresonant).

To the extent that the light-propagation direction is not perpendicular to $\mathbf{B}$ and the light polarization does not average to zero, the atomic oscillators can acquire a light induced frequency shift [13]. The present geometry reduces this light shift by at least a factor of 200 from our previous experiment where it was the dominant source of noise.

The light transmitted by each cell is detected by a photomultiplier which is sensitive only to UV. Each signal is amplified and fed into a pair of phase sensitive detectors (PSD's) which use a reference signal generated by a slotted wheel attached to the rotating polarizer. One PSD in each pair detects the component of the transmitted light that is in phase with the light polarization (V_1^{in}, V_2^{in}) where 1 and 2 denote cell 1 and cell 2, and the other detects the component that is 90° out of phase with the light polarization (V_1^{out}, V_2^{out}). Close to resonance (i.e., when $\omega \cong \omega_L$), V_1^{out} and V_2^{out} are nearly zero and approximately linear in $\omega - \omega_L$, so the sum of V_1^{out} and V_2^{out} is fed back to the B coils to keep $\omega \cong \omega_L$.

To cancel any residual magnetic field offset between the cells there is also an anti-Helmholtz coil that produces a magnetic field gradient along $\hat{\mathbf{z}}$ at the cells. The difference between V_1^{out} and V_2^{out} is held close to zero through feedback to these gradient coils. This gradient correction signal provides a measure of $\delta\nu$, the frequency difference between the cells. A change in this signal which is correlated with the electric field direction would be evidence for an EDM. The calibration of the gradient correction signal, 26 μHz/V, is determined by applying a known current through the anti-Helmholtz coil. The drift in magnetic field gradient was typically less than 1 nG/h (see Fig. 2).

The cells contain about 10^{-3} torr of mercury vapor to produce ≈70% absorption of the pumping light, and 300 torr of nitrogen buffer gas to increase the high-voltage

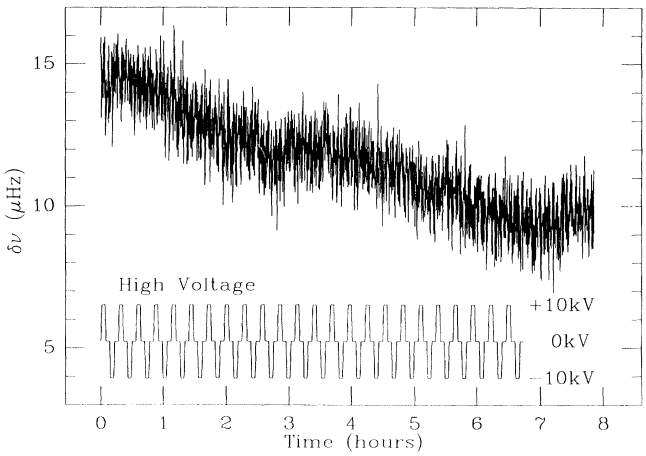

FIG. 2. Typical gradient correction data with high-voltage sequence included. No discontinuities were found in this 24 h run. Only part of the run is shown in order to make the HV flip sequence discernible.

(HV) breakdown potential within the cells. These cells, an improved version of our previous cells [4], required an extensive development [10]. We found that trace oxygen impurities must be removed from the buffer gas to prevent loss of Hg atoms through formation of HgO. In addition, hydrogen atoms accumulating on the walls of the cells relax the spins and limit their spin lifetime. Adding 5% CO to the buffer gas alleviated this problem because the CO reacts with the H in the presence of UV, stabilizing the spin relaxation lifetime (T_2) at about 45 s.

During a run the setting of the HV supply that generates $\mathbf{E}$ in the cells is changed in the sequence (HV+, HV0, HV−, HV0, HV+, ...). Each HV "dwell" is approximately 300 s, but there are magnetic fields produced by the charging currents, so only the final 50 s are used for the determination of the EDM value for that dwell. (Earlier times are used to look for possible systematic effects.) The frequency shift, $\delta\nu$, and other relevant parameters were monitored through about 200 successive reversals of $\mathbf{E}$ per run. The statistical uncertainty on $\delta\nu$ for a typical run is about 0.03 μHz which corresponds to $3 \times 10^{-27} e$ cm for one 24 h period when E =10 kV/cm.

The data we report here come from three data sets, which were taken over a 3-yr period. Data sets 1 and 2 have 88 and 98 one-day runs, respectively, but improvements in data set 3 allowed better precision with only 48 runs. The same pair of cells was used in data sets 1 and 3 and a different pair in data set 2. For set 3, the cell lifetimes were rejuvenated by gentle heating, yielding longer spin relaxation lifetimes (60 s). To identify possible systematic errors, many experimental parameters were reversed between runs: the phase of the pump-light modulation, the sign of ω for the pump-light modulation, the direction of $\mathbf{B}$, and the sign of the gradient correction current. In addition, the magnitude of $\mathbf{E}$ was toggled between 5 and 10 kV/cm.

Every 0.1 s a computer digitized the signals from 16 data channels. These include $\delta\nu$, the gradient correction signal; $\bar{\nu}$, the **B** correction signal; $V_1^{\rm in}$, $V_2^{\rm in}$, $V_1^{\rm out}$, and $V_2^{\rm out}$ defined above; $\mathcal{I}_1$ and $\mathcal{I}_2$, the average light intensity through each cell; and i_1, i_2, and i_m, the leakage currents across the two cells and to the cell holding vessel. Each 50 s of data was averaged, yielding 4 or 5 points per high-voltage dwell for subsequent analysis.

Figure 2 shows the raw $\delta\nu$ signal for a typical run with the HV dwells included. The analysis extracts the EDM signal, $\delta\nu(\mathbf{E})$, by removing the drifts in the raw data and correlating any frequency shifts with the electric field reversals. Occasional discontinuities in the $\delta\nu$ signal (caused by relaxation of the magnetic fields) were removed, reducing the total amount of data by $< 5\%$. An identical analysis was used to extract any signals of the form $\delta\nu(|\mathbf{E}|)$. Such correlations with $|\mathbf{E}|$ would be expected from a frequency shift which is quadratic in the applied **E** field. A pseudo-EDM signal, $\delta\nu(\mathbf{0}_{+-})$, was also sought by treating the HV0 dwell after HV+ as a pseudo "+" dwell and the HV0 after HV− as a pseudo "−" dwell. Such a signal might be expected, for example, if the HV surge currents were magnetizing the magnetic shields.

To mimic or cancel a true EDM in our system, any real or apparent frequency shift must be asymmetric in the two cells, linear in **E**, and must survive the experimental reversals described above. Leakage currents flowing across the cells have this signature if they produce a magnetic field that projects onto **B**. As the HV is ramped, surge currents of 2 nA flow across the cells. We examine the data taken immediately after the HV ramp and find no evidence that surge currents affect our final EDM value. Approximately 100 s after the HV is applied, i_1 and i_2 reach their steady state values of ≤ 2 pA. If this current were to flow in a complete loop around the cell the frequency shift of the atomic oscillators would be less than 0.5 nHz, a negligible value.

Other potential systematic effects include the quadratic Stark shift of the optical absorption line feeding through to an EDM signal, surge currents magnetizing the magnetic shields, external magnetic fields correlated with **E**, cross talk between different data channels in the computer, rf broadcasting of the HV supply, deviations of the light beam or changes in light polarization that are correlated with **E**, coupling of changes in the atomic polarization gradients to magnetic field gradients within the cells, and the Stark induced multipole interference that is linear in **E** [14]. Each of these possible systematic effects was considered and reduced to a level below the statistical uncertainty.

Changes in any data channel that are correlated with $\delta\nu(\mathbf{E})$ could be evidence of a systematic effect. We analyzed each data channel for the **E**, $|\mathbf{E}|$, and $\mathbf{0}_{+-}$ effects discussed above and looked for correlations between these results and the results for $\delta\nu(\mathbf{E})$. We found that for the 10 kV runs in data sets 1 and 2, $\delta\nu(\mathbf{E})$ was correlated with $\mathcal{I}_1(\mathbf{E})$ and $\mathcal{I}_2(\mathbf{E})$, but with opposite signs in the two data sets. We believe these correlations are produced from phase offsets between the reference to the phase detectors and the light modulation signal. In data set 3, where these phase shifts were eliminated, we found no such correlation. For the 10 kV runs in data set 1, there was a correlation between $\delta\nu(\mathbf{E})$ and $\delta\nu(|\mathbf{E}|)$. This correlation is troubling because a resolved signal (3σ) was found on $\delta\nu(|\mathbf{E}|)$ for these runs which could feed through to $\delta\nu(\mathbf{E})$ through imperfect reversal of the electric field.

Table I shows our results for each data set broken down into 10 kV and 5 kV subsets. One of the six $d(^{199}\mathrm{Hg})$ subsets (the 10 kV runs in data set 2) showed evidence of extra scatter with $\chi^2 \cong 1.4$. The rest of the $d(^{199}\mathrm{Hg})$ data, a total of 186 runs, showed good statistical behavior with an average χ^2 of 1.04. The errors given for the data subsets in Table I are either corrected for χ^2 or derived from the unweighted scatter, whichever produces the larger error in each case. The combined results shown in Table I are obtained by computing the weighted mean of the three data sets, with the 10 kV and the 5 kV results included separately. Because some potential systematic errors may be common to all three data sets, we do not assign a systematic error to each set. (We find that assigning such an error, and weighting the sets accordingly, changes the combined average by only a small fraction of the final error.) In the correlation analysis described above the only significant correction occurs with the correlation between $\delta\nu(\mathbf{E})$ and $\delta\nu(|\mathbf{E}|)$ in the 10 kV runs of data set 1. The possible shift in final central value is found to be $2.3 \times 10^{-28} e$ cm, and is subject to the same statistical error, $3.8 \times 10^{-28} e$ cm, as the central value itself. Combining the shift and associated statistical error in quadrature yields a systematic uncertainty of $4.4 \times 10^{-28} e$ cm, which we believe to be a conservative estimate of the possible effect that this correlation may have on the final result. No corrections to the central value are made. We find

$$d(^{199}\mathrm{Hg}) = -(2.7 \pm 3.8 \pm 4.4) \times 10^{-28} e\,\mathrm{cm}, \qquad (3)$$

TABLE I. Results for each data set and combined results with 5 and 10 kV/cm results included separately. The $\delta\nu(\mathbf{E})$ results are presented in terms of $d(^{199}\mathrm{Hg})$ as defined in Eq. (2), and are in units of $10^{-28} e$ cm. For convenience, the $\delta\nu(|\mathbf{E}|)$ and $\delta\nu(\mathbf{0}_{+-})$ effects are also in units of $10^{-28} e$ cm.

Set	HV	$d(^{199}\mathrm{Hg})$	$\lvert\mathbf{E}\rvert$	$\mathbf{0}_{+-}$
1	10 kV	7.4 ± 10.7	53.6 ± 19.1	1.9 ± 9.6
	5 kV	−20.1 ± 17.3	42.6 ± 20.3	25.2 ± 20.3
2	10 kV	−10.9 ± 7.4	0.6 ± 10.1	−10.0 ± 5.9
	5 kV	−5.5 ± 12.5	−12.5 ± 15.2	9.3 ± 11.6
3	10 kV	0.2 ± 6.2	−11.2 ± 9.2	−1.5 ± 6.3
	5 kV	4.8 ± 11.3	1.4 ± 20.9	−12.9 ± 12.6
	Ave.	−2.7 ± 3.8	2.2 ± 5.5	−3.1 ± 3.5

TABLE II. Upper limits (95% confidence level) on T-violating interactions set by the ^{199}Hg result reported here ($d < 1.3 \times 10^{-27} e\,\mathrm{cm}$), compared with the best current limits from other experiments.

T-violating parameters	Ref.	Limit from ^{199}Hg	Best limit from other work	
Hadronic:				
Schiff moment (Q_S)	a	$Q_S < 3 \times 10^{-11} e\,\mathrm{fm}^3$	$Q_S < 1 \times 10^{-9} e\,\mathrm{fm}^3$	TlF[e]
$i\eta G_F(\bar{n}n)(\bar{n}\gamma_5 n)/\sqrt{2}$	a	$\eta < 2 \times 10^{-3}$	$\eta < 2 \times 10^{-2}$	TlF[e]
$i\eta_q G_F(\bar{q}q)(\bar{q}\gamma_5 q)/\sqrt{2}$	a	$\eta_q < 5 \times 10^{-6}$	$\eta_q < 4 \times 10^{-5}$	Neutron[f]
QCD phase ($\bar{\theta}_{\mathrm{QCD}}$)	a,b,c	$\bar{\theta}_{\mathrm{QCD}} < 7 \times 10^{-10}$	$\bar{\theta}_{\mathrm{QCD}} < 4 \times 10^{-10}$	Neutron[f]
Supersymmetry ($\epsilon_q^{\mathrm{SUSY}}$)	b	$\epsilon_q^{\mathrm{SUSY}} < 1 \times 10^{-2}$	$\epsilon_q^{\mathrm{SUSY}} < 1 \times 10^{-2}$	Neutron[f]
Semileptonic:				
$iC_T G_F(\bar{n}\gamma_5\sigma_{\mu\nu}n)(\bar{e}\sigma^{\mu\nu}e)/\sqrt{2}$	a,d	$C_T < 2 \times 10^{-8}$	$C_T < 5 \times 10^{-7}$	TlF[e]
$iC_S G_F(\bar{n}n)(\bar{e}\gamma_5 e)/\sqrt{2}$	a	$C_S < 1 \times 10^{-6}$	$C_S < 2 \times 10^{-6}$	Tl[g]
Leptonic:				
Electron (d_e)	a	$d_e < 9 \times 10^{-26} e\,\mathrm{cm}$	$d_e < 1 \times 10^{-26} e\,\mathrm{cm}$	Tl[g]

[a]Reference [8], and references therein.
[b]Reference [9].
[c]The mean of several estimates is quoted here.
[d]Reference [15].
[e]Reference [7].
[f]Reference [2], where $d_n < 1 \times 10^{-25} e\,\mathrm{cm}$.
[g]Reference [5].

where the first error is statistical and the second systematic. This result can be used to set an upper limit on the possible size of the EDM of ^{199}Hg

$$d(^{199}\mathrm{Hg}) < 1.3 \times 10^{-27} e\,\mathrm{cm}\ (95\%\ \mathrm{confidence}), \quad (4)$$

where the limit is $|d(^{199}\mathrm{Hg})| + 1.7\sigma$ with σ given by the quadrature sum of the two errors shown in Eq. (3).

Table II shows the limits on various T-violating interactions set by our ^{199}Hg result, and for comparison includes limits set by other experiments as well. An atomic or molecular EDM could arise from an EDM distribution in the nucleus, from a T-violating force between electrons and nucleons, or from an intrinsic EDM of the electron itself, corresponding, respectively, to hadronic (quark-quark), semileptonic (electron-quark), or purely leptonic interactions as the chief source of T violation.

^{199}Hg is sensitive to hadronic interactions through its nuclear Schiff moment, Q_S, which measures the detectable, unshielded part of a nuclear EDM. A finite Schiff moment would reveal the presence of T-violating interactions between individual nucleons, and ultimately between the quarks in the nucleus. The table shows the limit on the Schiff moment and the derived limit on η, the T-violating nucleon interaction coefficient. The limit on η places important bounds on fundamental sources of T violation at the quark level, also shown in the table. For example, T-violating phases occur naturally in supersymmetric (SUSY) theories. It is expected that $\epsilon_q^{\mathrm{SUSY}} \approx 1$ if supersymmetry is broken near the electroweak energy scale [9], whereas $\epsilon_q^{\mathrm{SUSY}} < 10^{-2}$ according to both the ^{199}Hg and the neutron EDM experiments. ^{199}Hg is also sensitive to the semileptonic tensor-pseudotensor coupling between electrons and nucleons, as shown by the limit on C_T in the table, and somewhat less sensitive to the semileptonic scalar-pseudoscalar coupling or to an intrinsic EDM of the electron.

We thank E. Adelberger, J. Cederberg, I. Khriplovich, R. Morley, and L. Sorensen for help in various aspects of the experiment. The work was supported by National Science Foundation Grant No. PHY-9206408.

* Present address: Department of Physics, University of Montana, Missoula, MT 59812.

[1] J. H. Christenson, J. W. Cronin, V. L. Fitch, and R. Turlay, Phys. Rev. Lett. **13**, 138 (1964).
[2] K. F. Smith *et al.*, Phys. Lett. B **234**, 191 (1990).
[3] I. S. Altarev *et al.*, Phys. Lett. B **267**, 242 (1992).
[4] S. K. Lamoreaux, J. P. Jacobs, B. R. Heckel, F. J. Raab, and E. N. Fortson, Phys. Rev. Lett. **59**, 2275 (1987).
[5] K. Abdullah, C. Carlberg, E. D. Commins, Harvey Gould, and Stephen B. Ross, Phys. Rev. Lett. **65**, 2347 (1990).
[6] S. A. Murthy, D. Krause, Jr., Z. L. Li, and L. R. Hunter, Phys. Rev. Lett. **63**, 965 (1989).
[7] D. Cho, K. Sangster, and E. A. Hinds, Phys. Rev. Lett. **63**, 2559 (1989).
[8] I. B. Khriplovich, *Atomic Physics 11*, Proceedings of the Eleventh International Conference on Atomic Physics, Paris, 1988 (World Scientific, Singapore, 1989), p. 113; V. M. Khatsymovsky and I. B. Khriplovich, Phys. Lett. B **296**, 219 (1992).
[9] S. M. Barr, Int. J. Mod. Phys. A **8**, 209 (1993).
[10] J. P. Jacobs, Ph.D. thesis, University of Washington, 1991 (unpublished).
[11] S. K. Lamoreaux, Nucl. Instrum. Methods Phys. Res., Sect. A **284**, 43 (1989).
[12] A more complete discussion of the experiment is in preparation and will appear in a forthcoming publication.
[13] W. Happer, Rev. Mod. Phys. **44**, 169 (1972).
[14] S. K. Lamoreaux and E. N. Fortson, Phys. Rev. A **46**, 7053 (1992).
[15] A.-M. Mårtensson-Pendrill, Phys. Rev. Lett. **54**, 1153 (1985).